NÖHÜ Müh. Bilim. Derg. / NOHU J. Eng. Sci., 2023; 12(3), 743-751

Niğde Ömer Halisdemir Üniversitesi Mühendislik Bilimleri Dergisi
Niğde Ömer Halisdemir University Journal of Engineering Sciences

Araştırma makalesi / Research article

www.dergipark.org.tr/tr/pub/ngumuh / www.dergipark.org.tr/en/pub/ngumuh

Comparison of exponential and constant voltage based models of power LED driven by isolated CUK DC-DC converter

İzoleli DC-DC CUK konverter ile sürülen güç LED'inin üstel ve sabit gerilime dayalı modellerinin karşılaştırılması

Erdal Şehirli[1,*]

[1] *Kastamonu University, Electric and Electronic Engineering Department, 37150, Kastamonu, Türkiye*

Abstract

Design and application of LED driver with isolated CUK converter for 10W is realized in this paper especially for automotive purposes. The advantage of isolated CUK topology from conventional CUK topology is to have electrical isolation with supply and load and providing same polarity output. Besides, power LED models including constant voltage and exponential model are obtained and employed in simulation study. Furthermore, maximum current limitation of power LED is provided via dsPIC30f4011 microcontroller. Also, power switch is operated by 100 kHz switching frequency, and connection of the power LED driver to the source provided by LC with parallel damping filter, whose noise reduction shown by application as well. Thanks to the experimental set up and simulations, proving the desired results provided by the converter is shown by the measurement of LED current-voltage, input voltage-current. Simulation results also verifies application. Moreover, it is shown that exponential power LED model provides more accurate results than constant voltage model.

Keywords: Automotive, DC-DC, Isolated CUK, Power LED, Model

Öz

Bu çalışma, özellikle otomotiv uygulamaları için, 10 W'a kadar izoleli CUK dönüştürücü kullanan LED sürücünün tasarımı ve uygulaması gerçekleştirilmiştir. İzoleli CUK dönüştürücünün geleneksel CUK dönüştürücüye göre avantajı yük ve kaynak arasındaki izolasyon ve aynı polaritedeki çıkış gerilimidir. Ek olarak, karşılaştırma için, güç LED'inin sabit gerilim ve eksponansiyel modelleri çıkarılmıştır ve benzetimde kullanılmıştır. İlaveten, maksimum güç LED'i akım sınırlaması dsPIC30f4011 denetleyicisi ile sağlanmıştır. Bununla birlikte, güç anahtarı 100 kHz anahtarlama frekansında çalıştırılmıştır ve dönüştürücünün kaynağa bağlantısı, paralel bastırmalı LC filtre ile gerçekleştirilmiştir ve filtrenin gürültü azaltımı uygulama sonuçları ile gösterilmiştir. Deneysel uygulama ve benzetimler ile dönüştürücün istenilen sonuçları sağladığı, ölçülen LED akım-gerilimi, giriş-akım gerilimi ile gösterilmiştir. Uygulama sonuçları da benzetim üzerinden doğrulanmıştır. Ayrıca, eksponansiyel güç LED'i modelinin, sabit gerilim modeline göre daha doğru sonuçlar verdiği gösterilmiştir

Anahtar kelimeler: Otomotiv, DC-DC, Izoleli CUK, Güç LED'i, Model

1 Introduction

Illumination is very critical topic in electrical engineering. To provide illumination, recently power LEDs have been becoming so popular due to the having higher lighting efficiency than other sort of traditional devices such as high-intensity discharge (HID) and halogen bulbs employed especially in automotive purpose. On the other hand, power LEDs require energy in DC power form. To adjust brightness of the power LEDs, this DC power should be variable. The best way is to use a DC-DC converter for this purpose. Although there are a lot of converter topologies like boost, buck, buck-boost DC-DC etc., in automotive field it is desirable for converter having electrical isolation, and providing same polarity output voltage with higher or lower than input voltage. Therefore, isolated CUK converter is a good choice for power LED driver as a car headlighting in automotive application. Besides, isolated CUK converter can provide better current wave forms because of having inductors at output and input sides.

Some studies related with the topic for automotive lighting are listed as follows; [1] presents the comparison of the lighting methods in automotive by emphasizing advantage of power LEDs. [2] presents dual phase PWM LED driver, [3] proposes series resonant non isolated converter, [4] presents buck-boost converter in and [5] offers four switch buck-boost. For wide input variation [6] presents H bridge converter. Isolated CUK converter is presented in [7] with high frequency application without considering LED models and input current ripple reduction. [8] presents flyback converter. [9] realizes synchronous buck-boost ZVS converter by using GaN MOSFET. LED driver based on forward-Flyback is presented in [10]. Zeta-boost based converter is proposed in [11].

In addition, isolated CUK converter design, and analysis is first introduced in [12]. As a LED driver, isolated CUK converter for providing higher power factor, is given in [13]

* Sorumlu yazar / Corresponding author, e-posta / e-mail: esehirli@kastamonu.edu.tr (E. Şehirli)
Geliş / Recieved: 24.01.2023 Kabul / Accepted: 30.05.2023 Yayımlanma / Published: 15.07.2023
doi: 10.28948/ngumuh.1241948

with simulation study and in [14] with application. Also, in [15] SiC MOSFET is used in isolated CUK LED driver for higher power factor application.

Recent studies have also investigated led lighting on automotive LED lighting applications, some of them is as follows. [16] presents buck-boost converter for matrix headlights. [17] proposes hybrid resonant converter for as a LED driver. [18] realizes adaptive control system considering thermal calibration, [19] designs robust PI controller. [20] investigates thermal degradation of solder interconnection of power LED, [21] examines thermal performance of power LED by experimentally. For high frequency application GaN switch is used in [22].

In this paper, LED driver application employing DC-DC isolated CUK converter as an electrical vehicle headlight up to 10W power is realized. Besides, models of power LED based on exponential and constant voltage are obtained, they are compared by simulations and application. Also, for power LED maximum current limitation, a current sensor is used with dsPIC30F4011 microcontroller. Thanks to the experimental set up and simulations, proving the desired results provided by the converter is shown by the measurement of LED current-voltage, input voltage-current. In addition, simulation results verify the application. Further, it can be concluded that exponential model of power LED gives more accurate results than constant voltage model by the comparisons. Moreover, ensuring continuous input current and reducing high frequency noises, LC with parallel damping input filter is used and its noise reduction shown by frequency spectrum analysis.

2 Modeling of power LED

Power LED characteristic of current-voltage is obtained by multimeter as shown in Fig.1 for the study as in [23].

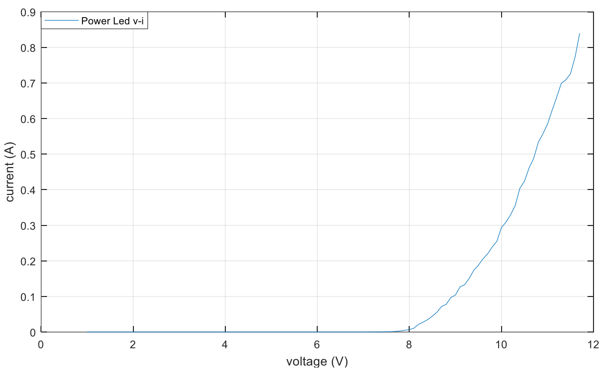

Figure 1. Power LED current-voltage characteristic

By the characteristic in Fig.1, model of power LED can be expressed with the diode equation in Equation (1) as in [24].

$$I_D = I_s(e^{\frac{V_D}{nV_T}} - 1) \approx I_s e^{\frac{V_D}{nV_T}} \tag{1}$$

In (1), V_D is diode voltage, V_T is thermal voltage, I_s is reverse saturation current, n is constant. By using MATLAB curve fitting tool, Fig.1 and Equation (1), as shown in Fig.2, power LED exponential model is obtained in Equation (2) as in [15].

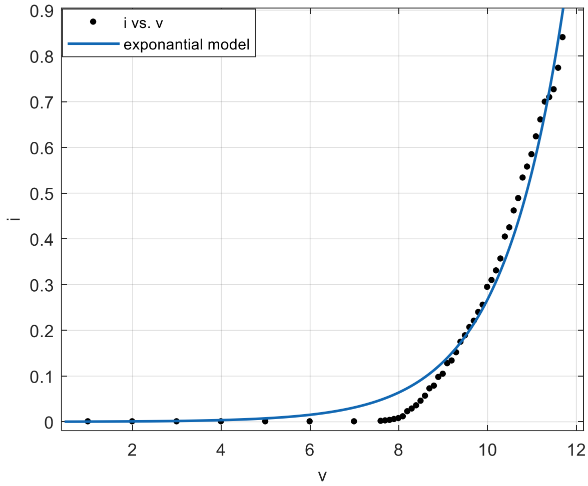

Figure 2. Curve fitting of current-voltage characteristic

$$f(x) = ae^{bx} = 0.0002113e^{0.7145x} \tag{2}$$

By Equation (2), it can be determined that the I_s equals to 0.0002113A and $1/nV_T$ equals to 0.7145 (1/V). By using the results, power LED exponential model is drawn in Fig.3 as in [15]. Although, power LED exponential model for different power LED is obtained in [15], model comparison is not presented.

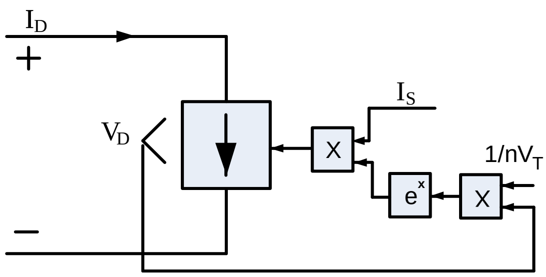

Figure 3. Power LED exponential model

In addition, by using average resistor value (r_{av}) as in normal diode in [23], power LED constant voltage model is derived in Fig.4. By using the power LED i-v characteristic in Fig.4, r_{av} can be calculated as 4.88 Ω and threshold voltage of power LED is determined as 7.6 V as in [23].

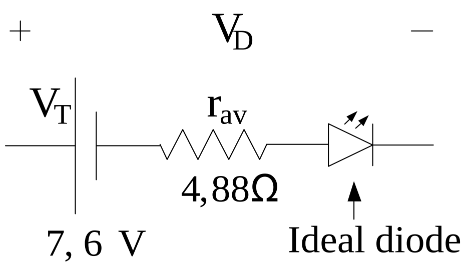

Figure 4. Power LED constant voltage model

3 Isolated CUK converter

Fig.5 depicts isolated CUK converter topology. The inductors used in the converter have coupled structure. Also, converter has three capacitors, switch, diode, and high frequency transformer as in [15].

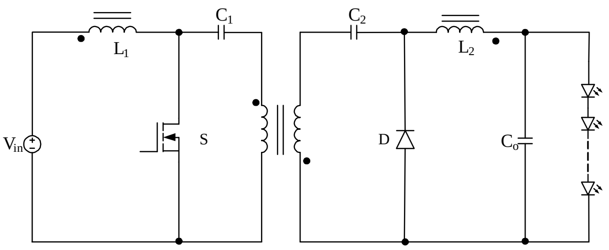

Figure 5. Isolated CUK converter

High frequency transformer is the main difference of the converter regarding to traditional CUK converter. Besides, splitted intermediate capacitors are placed at secondary and primary sides. Isolated CUK converter operation principle can be explained regarding to switch positions. At the switch on interval, L_1 is charged, and by high frequency transformer, energy of C_1 is transferred to C_2, also energy of L_2 is transferred to load via D. At the switch off interval, by input source and L_1, C_1 is charged and energy of C_2 is transferred to load and L_2. Isolated CUK converter equivalents are shown in Fig.6 regarding to switch positions as in [15].

By using Equation (3-7), isolated CUK converter components are selected as in [14].

$$L_1 = \frac{R_L(1-D)^2}{2Df_s n^2} \tag{3}$$

$$L_2 = \frac{R_L(1-D)}{2f_s} \tag{4}$$

$$C_1 = \frac{V_{in} n^2 D^2}{(1-D)\Delta V_{C1} f_s R_L} \tag{5}$$

$$C_2 = \frac{V_o D}{\Delta V_{C2} f_s R_L} \tag{6}$$

$$C_0 \geq \frac{V_o(1-D)}{8L_2 \Delta V_{C0} f_s^2} \tag{7}$$

Furthermore, DC-DC converters are generally operated by high frequency, and it needs to use an input filter to avoid high frequency noise and possible discontinuous input current. In this paper, isolated CUK converter is operated by 100kHz switching frequency, therefore an input LC filter is used. In Fig.7 the filter circuit is shown.

In Fig.7, L_f, C_f are filter capacitor, inductor. R_d, C_d are damping capacitor and resistor to provide damping of the filter. By using Equation (8-11), LC filter can be designed as in [23, 25].

$$L_f = \frac{1}{(2\pi 0.1 f_{sw})^2 C_f} \tag{8}$$

$$R_{in} \gg \frac{L_f}{C_f R_d} \tag{9}$$

$$C_f = nC_d \tag{10}$$

$$R_d = \frac{n_f + 1}{n_f} \frac{L_f}{2\zeta\sqrt{L_f C_f}} \tag{11}$$

Equation (12) presents the filter transfer function. By adding values used in the paper, the bode diagram of the filter is depicted in Fig.8, showing that the filter has 49.79 dB/decade attenuation. Also, peak magnitude is 33.1 dB at 833 rad/s cross over frequency.

$$T(s) = \frac{sR_dC_d+1}{s^3R_dC_dC_fL_f+s^2(R_dC_fL_f+R_dC_dL_f)+sR_dC_d+1} \tag{12}$$

4 Simulations and application

Firstly, simulation studies are realized in order to make a comparison of power LED models. Fig.9 gives the simulation circuit.

In the first simulation, as a load, power LED constant voltage model in Fig.4 is used. Fig.10-12 give simulation results. Fig.10 shows voltage of power LED, PWM, input voltage and input current. At the operating point, duty cycle is 0.47, power LED voltage is 11.7 V, and input current is 0.93A, input voltage is 12.8V. Fig.11 gives simulation results showing voltage of input, PWM, power LED voltage and current of power LED for constant voltage model. Power LED current is 0.84 A.

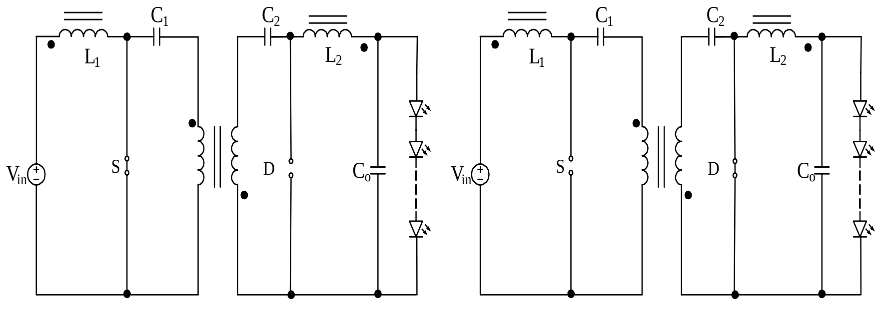

Figure 6. Switch on and off equivalents of the converter

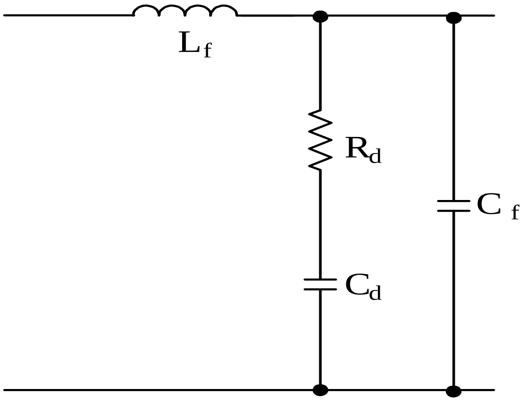

Figure 7. LC input filter

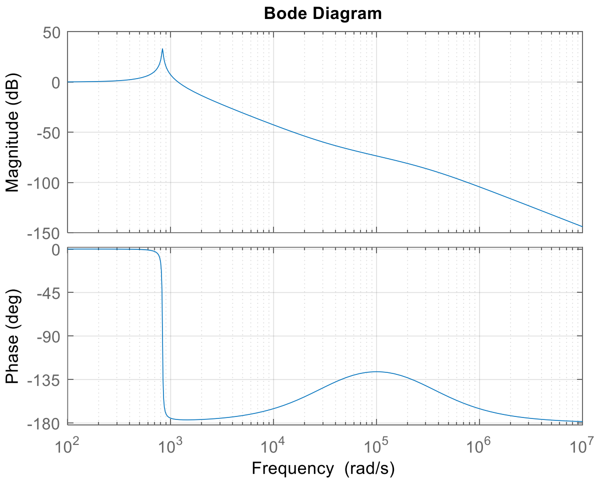

Figure 8. Bode diagram of the filter

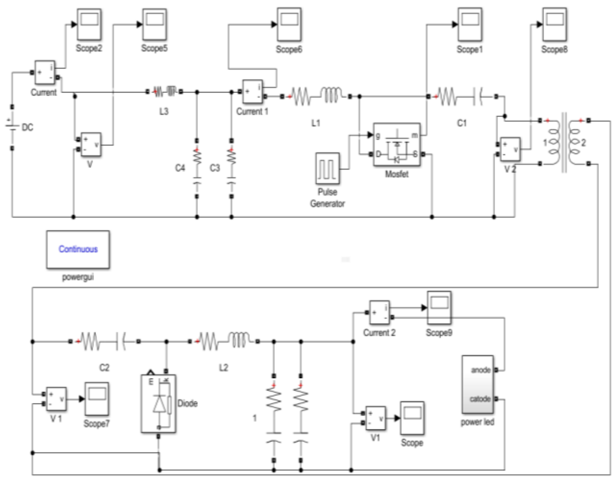

Figure 9. Simulation diagram of power LED driver with isolated CUK converter

Fig.12 gives simulation results showing voltage of power LED, PWM, input and L_1 current for constant voltage model. L_1 current has 2.24 A maximum value.

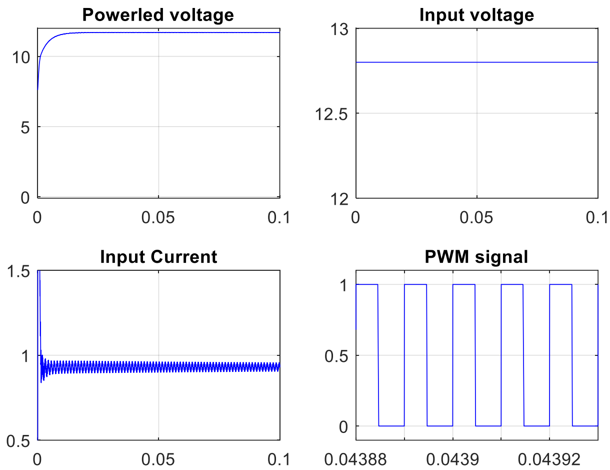

Figure 10. Voltage of LED, PWM, input voltage and current for constant voltage

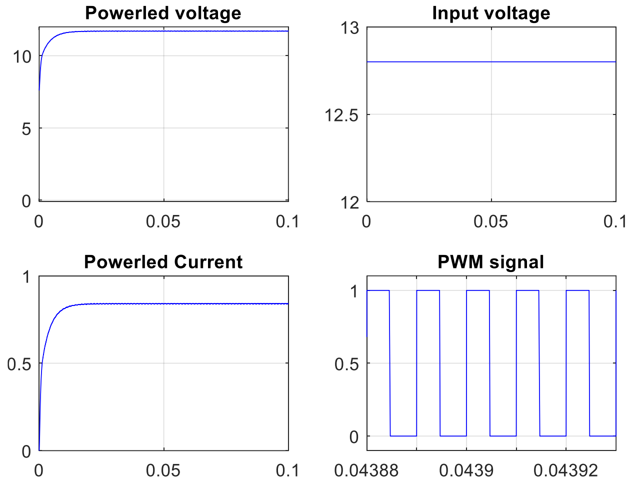

Figure 11. Voltage of power, input voltage, power LED current, PWM for constant voltage model of power LED

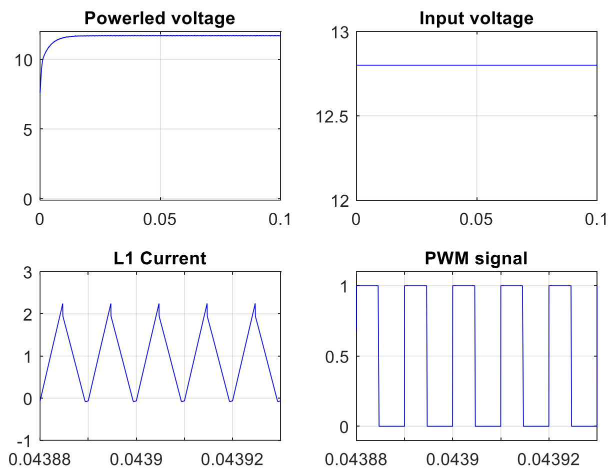

Figure 12. Voltage of power LED, input, PWM, and L_1 for constant voltage model

The simulation is also realized for exponential model of power LED as a load. Besides, Fig.13-15 give simulation results. Fig.13 shows voltage of power LED, input voltage, PWM, and input current. In addition, voltage of power LED is measured as 11.61 V, input current is 0.94A for operating point having 0.47 duty cycle and input voltage is 12.8.

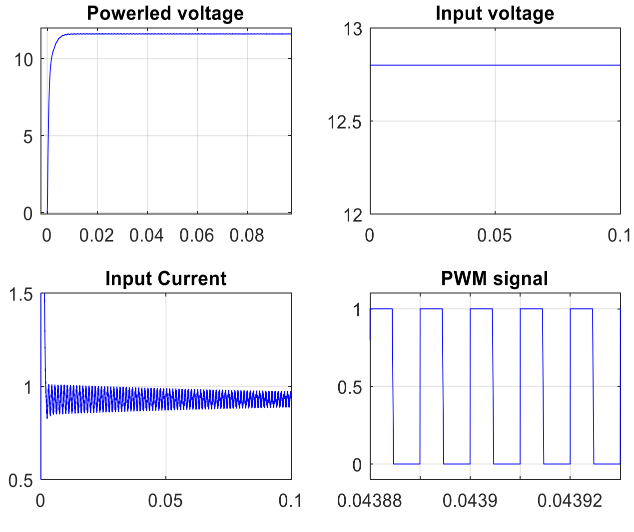

Figure 13. Voltage of power LED, input voltage, PWM, input current for exponential model

Fig.14 gives simulation results showing voltage of power LED, input voltage, PWM, and power LED current, for exponential model. Power LED current is 0.846 A.

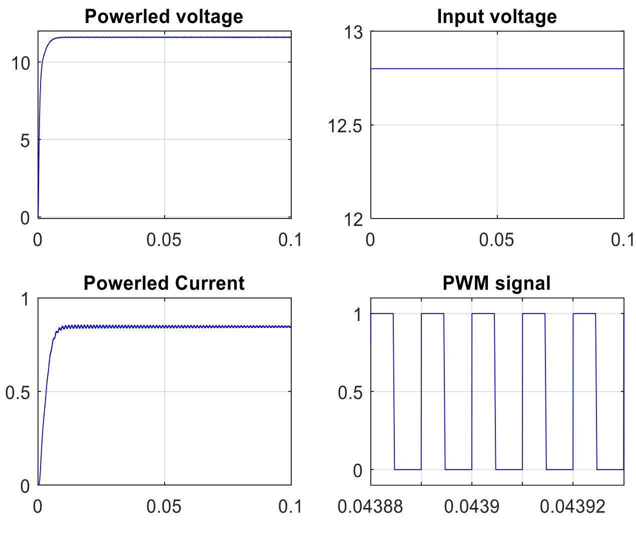

Figure 14. Voltage of power LED, input voltage, PWM and power LED current for exponential model

Fig.15 gives simulation results showing voltage of power LED, input voltage, PWM, and L_1 current for exponential model. L_1 current has 2.25 A maximum value.

LED driver application with isolated CUK converter is carried out by using dsPIC30f4011 microcontroller, ACS712 current sensor, IRF540N MOSFET, MUR820 diode. Fig.16a shows application set up. By using TPP0201 voltage, A622 current probes and TPS2024B oscilloscope, measurements are conducted. Input voltage of the converter is chosen as 12.8 V and as a load 10 W COB power LED is used. Also, L_1 and L_2 inductors are wounded as coupled meaning in the same core.

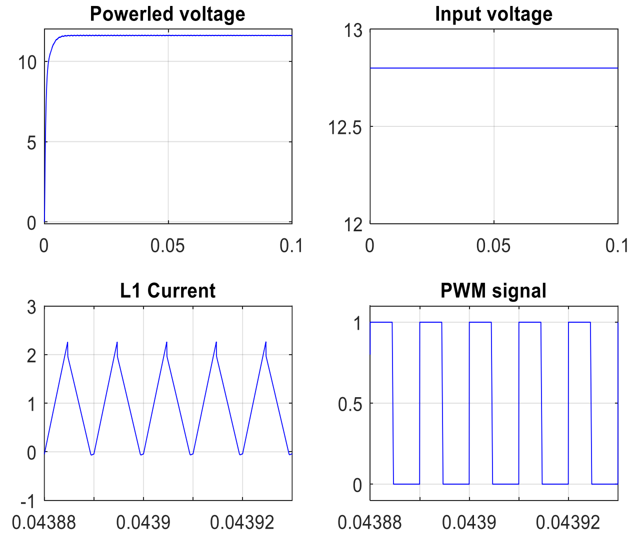

Figure 15. Voltage of power LED, input, PWM, L_1 current for exponential model

Table 1. lists values of components in the application. Fig.17 gives LED driver with isolated CUK converter application circuit. Power LED maximum current (I_{LED}) limitation is provided by ACS712, and V_{ref} is used to adjust illumination level.

In Fig.18, PWM signal, voltage of power LED, input current-voltage is shown. PWM is set to 0.47, power LED voltage is 11.3-11.4 V. Input current is 0.969 A. Input voltage is 12.8 V.

Table 1. Passive components in the application

L_1	L_2	C_1	C_2	C_0	n
26μH	35.6μH	20μF	20μF	940μF	1
L_f	C_f	C_d	R_d	f_{sw}	
12.67μH	22μF	4.7μF	7.5Ω	100kHz	

PWM signal, voltage of LED, L_1 current, and input voltage are shown in Fig.19, respectively. L_1 current mean value is 0.922 A and it has 5 A ripple value.

PWM, voltage of LED, LED current, input voltage is presented in Fig.20. LED current mean value is 0.791 A.

L_1 current frequency spectrum is shown in Fig.21. The current has higher peak magnitude 58 dB at switching frequency and 34 dB at 200 kHz, 33 dB at 300 kHz and 23 dB at 400 kHz.

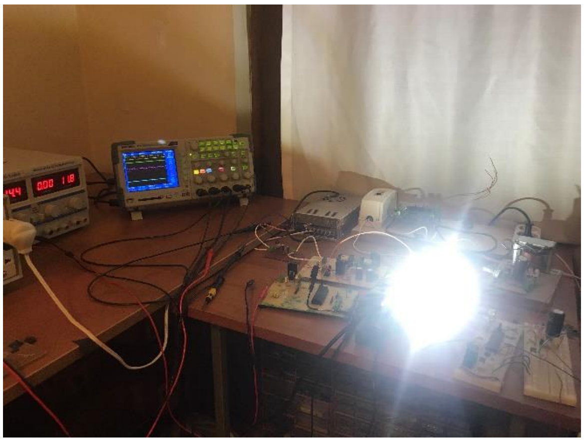

(a)

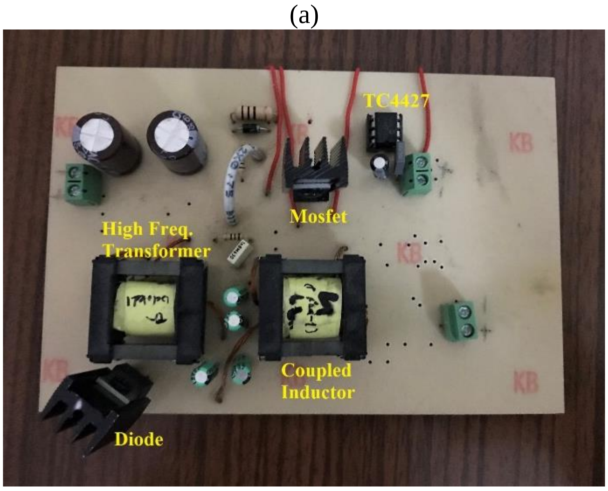

(b)

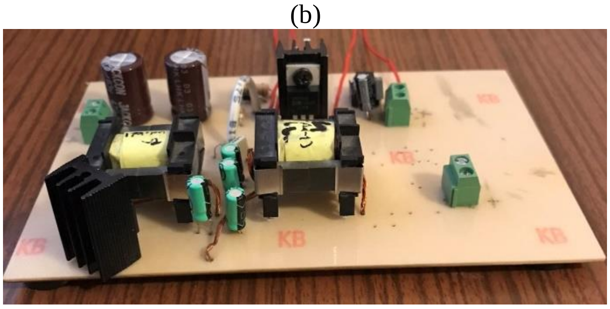

(c)

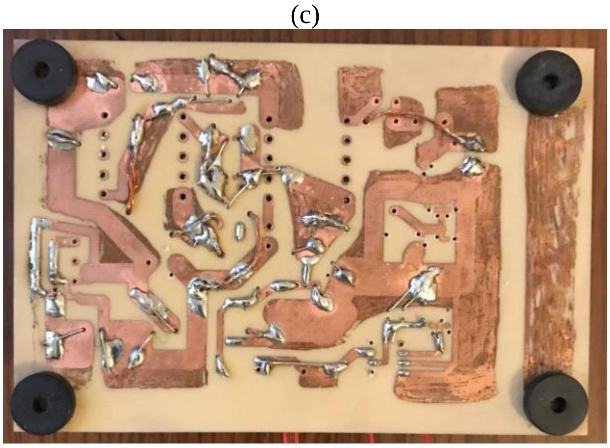

(d)

Figure 16. a) Laboratory environment, b) the converter, c) PCB side view d) PCB bottom view

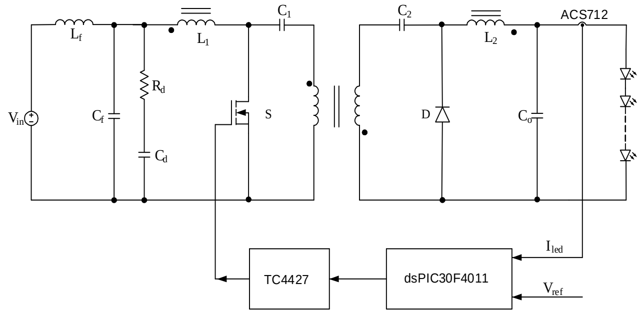

Figure 17. LED driver with isolated CUK converter application structure

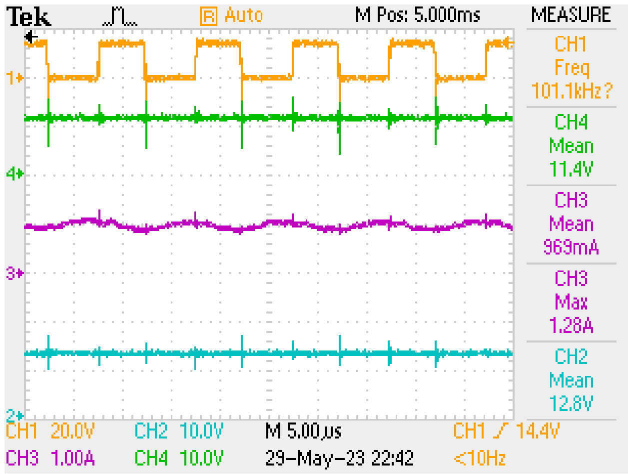

Figure 18. PWM, voltage of LED, input current-voltage

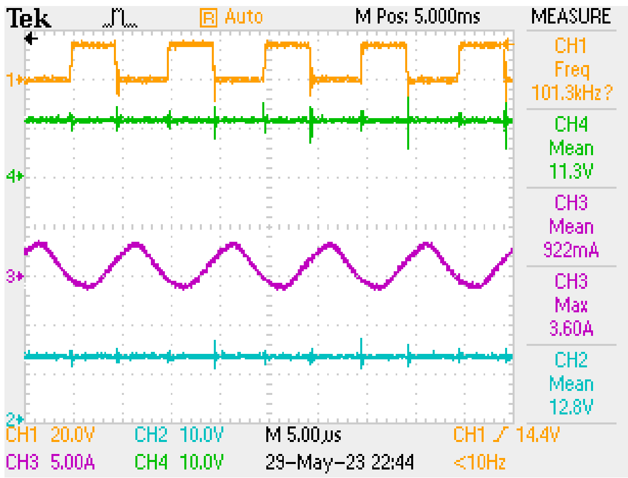

Figure 19. PWM, voltage of LED, L_1 current, and input voltage

Input current frequency spectrum with input filter is shown in Fig.22. By the filter, the peak magnitudes are reduced to 29 dB at 100 kHz, 10 dB at 200 kHz, 10 dB at 300 kHz and 13 dB at 400 kHz.

It is seen by Fig.21-22., the noise on the input current is reduced by using LC with parallel damping.

Fig.23 gives comparison of power LED voltage versus duty cycle. Application, constant voltage model and exponential model results are compared.

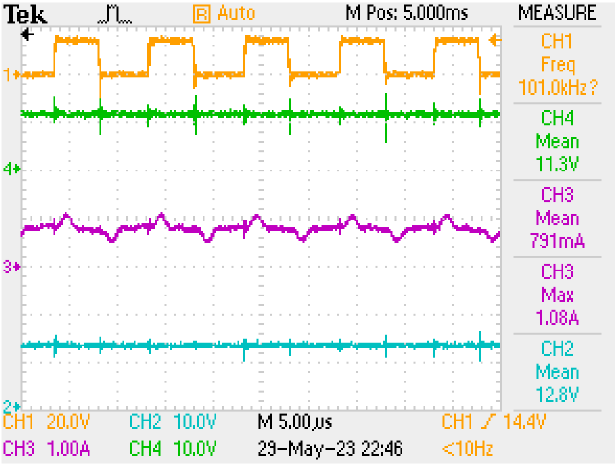

Figure 20. PWM, voltage of LED, LED current, input voltage

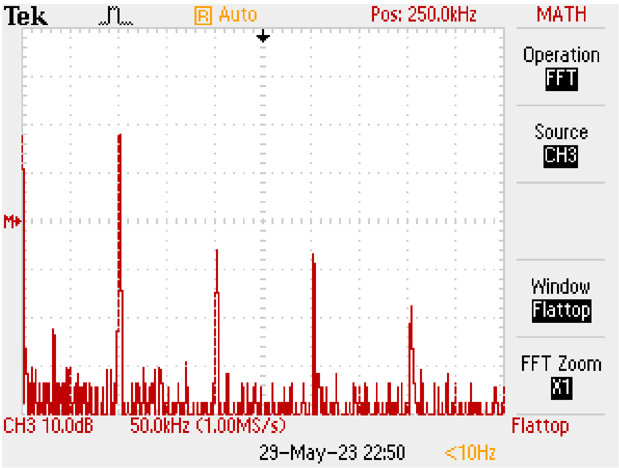

Figure 21. L_1 current frequency spectrum without input filter

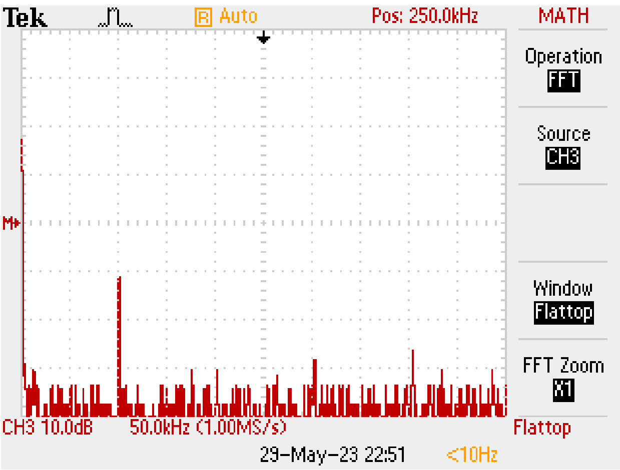

Figure 22. Input current frequency spectrum with input filter

Constant voltage model has linearly changing characteristic. However, exponential model gives better results at close to operation point and at lower values. Also, voltage variation of the exponential model is parallel for other values with application.

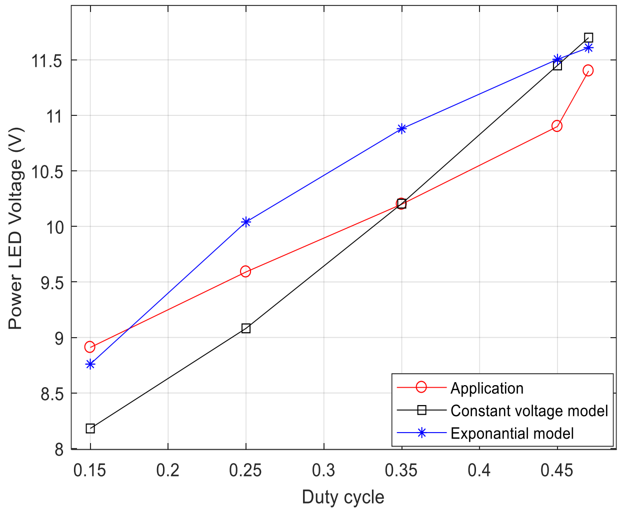

Figure 23. Comparison of power LED voltages

Fig. 24 gives comparison of power LED current versus duty cycle. Application, constant voltage model and exponential model results are compared. By Fig. 24, exponential model gives closer results to the application than constant voltage model.

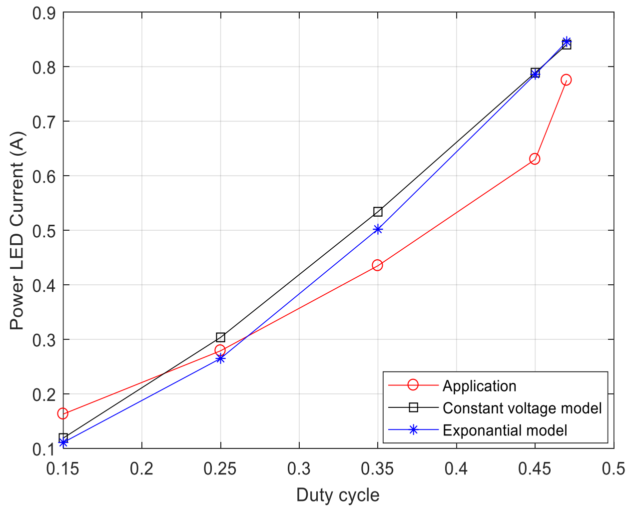

Figure 24. Comparison of power LED currents

Some relevant studies realized in the literature are compared in Table 2, regarding to switch number, isolation, power level, efficiency, operation frequency, output voltage. It can be concluded that presented study ensures moderate results with respect to the literature. Because the power level of the study is low, efficiency is obtained as 72% at applications and 82% at simulations. Besides, advantages of the topology used here are switch number and isolation capability. On the other hand, in the presented study, power LED models are compared which is not presented in literature.

Table 2. Comparison of the studies in literature

	Switch Nb	Isolation	Power (W)	Eff. (%)	Freq.	Output Voltage (V)
[2]	4	No	7.2 Dim.	94.7	1MHz	6 Dim.
[3]	4	No	22.77	94.2	200 kHz	22.5
[5]	4	No	25	82	500 kHz	25.6
[7]	1	Yes	15	89.6	1.8 MHz	up to 30
[26]	1	No	36	90.9	1MHz	120
Pres.	1	Yes	10	Up to 82	100 kHz	12

5 Conclusion

Having electrical isolation is the key advantage of isolated CUK converter for automotive purposes. In this paper, power LED driver application with isolated CUK converter for automotive purpose as an electrical vehicle headlight is realized. The application is conducted for up to 10W power, and the converter efficiency at 90% load is obtained as 72% by application and 82% by simulations. Furthermore, by using LC with damping input filter, ripple on the input current is reduced around 400mA. Also, LED current is obtained with small ripples. Besides, by using a current sensor, power LED maximum current is limited. In addition, constant voltage and exponential model of power LED are derived and compared by simulations and application. By comparisons, it can be concluded that exponential model of power LED ensures better results than constant voltage model for power LED voltage and power LED current. Also, simulation results verify the application result.

As a future work, the applied LED driver will be placed in an electrical vehicle and a current control algorithm will be added instead of limiting peak current.

Conflict of interest

The author declares no conflict of interest.

Similarity rate (iThenticate): 7%

References

[1] J. J. Santaella, S. Rodriguez-Bolivar, L. Puga-Pedregosa, A. Gonzalez and F. M. Gomez-Campos, High-Luminance QD-LED device with digital and dynamic lighting functions for efficient automotive systems. IEEE Photonics Journal, 14 (2), 1917610, 2022. https://doi.org/10.1109/JPHOT.2022.3155650.

[2] Y. Qu, W. Shu, J. S. Chang, A. Gonzalez-Rico, M. MarinGonzalez and F. M. Gomez-Campos, A Low-EMI, high-reliability PWM-based dual-phase LED driver for automotive lighting. IEEE Journal of Emerging and Selected Topics in Power Electronics, 6 (3), 1179-1189, 2018. https://doi.org/10.1109/ JESTPE.2018.2812902.

[3] V. K. S. Veeramallu, S. Porpandiselvi and B. L. Narasimharaju, A nonisolated wide input series resonant converter for automotive LED lighting system, IEEE Transactions on Power Electronics, 36 (5), 5686–5699, 2021. https://doi.org/10.1109/ TPEL.2020.3032159.

[4] J. Yao, S. Wang, and Z. Luo, Modeling and reduction of radiated EMI in non-isolated power converters in automotive applications. IEEE Applied Power Electronics Conference and Exposition (APEC), page 385-392, New Orleans, US, 15-19 March 2020.

[5] Y. Qin, S. Li and S. Y. Hiu, Topology-transition control for wide-input-voltage-range efficiency improvement and fast current regulation in automotive LED applications, IEEE Transactions on Industrial Electronics, 64 (7), 5883–5893, 2017. https://doi.org/ 10.1109/TIE.2017.2686304.

[6] A. Sureshkumar, and R. Gunebalan, Design and implementation of single switch control DC-DC converter with wide input variation in automotive LED lighting, International Transactions Electrical Energy Systems, 31 (4), 1–22, 2020. https://doi.org/10.1002/2050-7038.12776.

[7] A. Sepahvand, M. Doshi, V. Yousefzadeh, J. Patterson, K. K. Afridi, and D. Maksimovich, Automotive LED driver based on high frequency zero voltage switching integrated magnetics CUK converter. IEEE Energy Conversion Congress and Exposition (ECCE), page 1-8, Milwaukee, US, 18-22 September 2016.

[8] M. A. Juaraez, J. M. Sosa, G. Vazquez, R. Santillan, and I. Villanueva, Reliability analysis of a flyback converter for automotive applications. 14th International Conference on Power Electronics (CIEP), page 83-88, Cholula, Mexico, 24-26 October 2018.

[9] Q. Cheng and H. Lee, A high-frequency non-isolated ZVS synchronous buck-boost LED driver with fully-integrated dynamic dead-time controlled gate drive. IEEE Applied Power Electronics Conference and Exposition (APEC), pp. 419-422, San Antonio, US, 04-08 March 2018.

[10] J. W. Kim, J. P. Moon and G. W. Moon, Analysis and design of a single-switch forward-flyback two-channel led driver with resonant-blocking capacitor, IEEE Transactions on Power Electronics, 31 (3), 2314–2323, 2016. https://doi.org/10.1109/ TPEL.2015.2432458.

[11] P. Giannelli, L. Capineri, G. Calabrese, G. Frattinni and M. Granato, A reduced output ripple step-up DC-DC converter for automotive LED lighting. 13th Conference on Ph.D. Research Microelectronics and Electronics (PRIME), pp 329-332, Giardini Naxos, Italy, 12-15 June 2017.
[12] R. D. Middlebrook and S. CUK, Isolated and multiple output extensions of a new optimum topology switching dc to dc converter. IEEE Power Electronics Specialist Conference, pp 256-264, New York, US, 13-15 June 1978.
[13] J. R. Nolasco, G. M. Soarez and H. A. C. Braga, High power factor converter for led drivers based on isolated CUK topology. Simposio Brasileiro de Sistemas Eletricos, pp. 1-6, Niteroi, Brazil, 12-16 May 2018.
[14] S. Pal, B. Singh, A. Shrivastava, A. Chandra and K. Al-Haddad, Improved power quality opto-couplerless CUK converter for flickerless led lighting. IEEE Energy Conversion Congress and Exposition (ECCE), pp. 3239-3246, Montreal, Canada, 20-24 Sept 2015.
[15] E. Şehirli and Ö. Üstün, Design and implementation of high-power factor isolated ĆUK converter-based LED driver with SiC MOSFET. Electrical Engineering, 105, 465-476, 2023. https://doi.org/10.1007/s00202-022-01679-1.
[16] J. Moon, J. Lee, K. Javed, J. Hong, and J. Roh, Concurrent current and voltage regulated buck–boost converter for automotive LED matrix headlights. IEEE Transactions on Power Electronics, 38 (5), 6015-6023, 2023. https://doi.org/ 10.1109/TPEL.2023.3243303.
[17] N. Molavi, and H. Farzanehfard, Load-independent hybrid resonant converter for automotive LED driver Applications. IEEE Transactions on Power Electronics, 37 (7), 8199-8206, 2022. https://doi.org/ 10.1109/TPEL.2022.3144640.
[18] J. Lee, S. S. Kwak, and Y. S. Kim, Temperature-aware adaptive control for automotive front-lighting system. IEEE Access, 10, 73269-73277, 2022. https://doi.org/ 10.1109/ACCESS.2022.3189176.
[19] A. Sureshkumar, and R. Gunabalan, Design of robust guaranteed margin stability region PI controller for automotive LED lighting with parameter uncertainty. IEEE Access, 10, 15657-15670, 2022. https://doi.org/ 10.1109/ACCESS.2022.3146392.
[20] M. Schmid, A. Zippelius, A. Hanß, S. Böckhorst, and G. Elger, Investigations on High-Power LEDs and Solder Interconnects in Automotive Application: Part I—Initial Characterization. IEEE Transactions on Device and Materials Reliability, 22 (2), 175-186, 2022. https://doi.org/ 10.1109/TDMR.2022.3152590.
[21] I. L. Ngo, S. Bang, and B. J. Lee, Experimental study on thermal management of surface mount device–LED chips towards applicability in a headlamp of modern cars. Applied Thermal Engineering, 221, 119946, 2023. https://doi.org/ 10.1016/j.applthermaleng.2022.119846
[22] Y. H. Choi, H. J. Choi, and J. J. Yun, Study on 2 MHz GaN-based light-emitting diode driver for automotive headlamps. Journal of Electrical Engineering & Technology, 18, 249-260, 2023. https://doi.org/10.1007/s42835-022-01206-z.
[23] E. Şehirli, Comparison of DC-DC Sepic, CUK and flyback converters based led drivers. Light&Engineering, 28 (1), 99-107, 2020. https://doi.org/10.33383/2018-70.
[24] R. Boylestad, and L. Nastalsky, Electronic devices and circuit theory. Pearson, New Jersey, 2013.
[25] M. Sclocchi, Input filter design for switching power supplies. Texas Instruments, Texas, US, SNVA538, 2011.
[26] Y. Wang, S. Gao, and D. Xu, A 1-MHz-modified SEPIC with ZVS characteristic and low-voltage stress. IEEE Transactions on Industrial Electronics, 66 (5), 3422-3426, 2019. https://doi.org/ 10.1109/TIE.2018.2851974 .